



**IJBEM**

# **International Journal of Bioelectromagnetism**

Proceedings of the 11<sup>th</sup> International Conference on Bioelectromagnetism

23-25 May 2018, Aachen, Germany

Vol. 20, No. 1, 2018



# Proceedings of the 11<sup>th</sup> International Conference on Bioelectromagnetism

23-25 May 2018, Aachen, Germany

## Organizing Committee for ICBEM 2018 in Aachen

Prof. Steffen Leonhardt, RWTH Aachen University, Germany  
Prof. Jaakko Malmivuo, Technische Universität Berlin, Germany  
Dr. Marian Walter, RWTH Aachen University, Germany  
Benjamin Hentze, RWTH Aachen University, Germany  
Markus Lüken, RWTH Aachen University, Germany

## Scientific Committee for ICBEM 2018 in Aachen

Prof. Petri Ala-Laurila, University of Helsinki, Finland  
Prof. Martin Arthur, Washington University in St. Louis, USA  
Prof. Fabio Babiloni, Sapienza University of Rome, Italy  
Prof. Panagiotis Bamidis, Aristotle University of Thessaloniki, Greece  
Prof. Wenxi Chen, University of Aizu, Japan  
Prof. Catherine Disselhorst-Klug, RWTH Aachen University, Germany  
Prof. Olaf Dössel, Karlsruhe Institute of Technology, Germany  
Prof. Bobby George, Indian Institute of Technology Madras, India  
Prof. Jens Haueisen, Ilmenau University of Technology, Germany  
Prof. Craig Henriquez, Duke University, North Carolina, USA  
Prof. Risto Ilmoniemi, Aalto University, Finland  
Dr. Jayaraj Joseph, Indian Institute of Technology Madras, India  
Prof. Jukka Lekkala, Tampere University of Technology, Finland  
Prof. Thomas Lenarz, Medical University of Hannover, Germany  
Dr. Mohanasankar Sivaprakasam, Indian Institute of Technology Madras, India  
Prof. Rob MacLeod, University of Utah, Salt Lake City, USA  
Prof. Ratko Magjarevic, University of Zagreb, Croatia  
Prof. Vaidotas Marozas, Kaunas University of Technology, Lithuania  
Prof. Fernando Seoane Martínez, University of Borås, Sweden  
Prof. Mart Min, Tallinn University of Technology, Estonia  
Prof. Reinhold Orglmeister, Technische Universität Berlin, Germany  
Prof. Günter Rau, RWTH Aachen University, Germany  
Prof. Frank Sachse, University of Utah, USA  
Prof. Rosalind Sadleir, Arizona State University, USA  
Dr. Benjamin Sanchez, Harvard Medical School, Boston, USA  
Prof. Leif Sörnmo, Lund University, Sweden  
Prof. Bart Vanrumste, KU Leuven, Belgium  
Prof. Guang-Zhong Yang, Imperial College London, UK

## Introductory Words from the Editorial Board

The International Society for Bioelectromagnetism (ISBEM) was founded in 1996 in order to offer an exchange platform for researchers from all over the world regarding advances in bioelectromagnetism. Therefore, the society sponsors the biennially organised international congresses on bioelectromagnetism, starting from 1996. The first International Conference on Bioelectromagnetism (ICBEM) has been held in Tampere, Finland in 1996. After that, the ICBEM conference took place in Melbourne (1998), Bled (2000), Montreal (2002), Minneapolis (2005), Aizu (2007), Rome (2009), Banff (2011), Geneva (2013) and Tallinn (2015). Following the fundamental idea of the ISBEM, the ICBEM provides a platform for researchers all over the world to share their experience regarding their work in the broad field of bioelectromagnetism, which includes:

- The behavior of excitable tissue (the sources)
- The electric currents and potentials in the volume conductor
- The magnetic field at and beyond the body
- The response of excitable cells to electric and magnetic field stimulation
- The intrinsic electric and magnetic properties of the tissue.

This year, we are very happy to welcome all participants to the 11<sup>th</sup> International Conference on Bioelectromagnetism in Aachen, Germany. In 2018, the ICBEM will be jointly held together with the 13<sup>th</sup> Russian-German Conference on Biomedical Engineering (RGC) hosted by the Philips Chair for Medical Information Technology (MedIT) at RWTH Aachen University. As regarding for the editorial board, we would like to thank all participants contributing to ICBEM & RGC 2018 with their research and hope the conference to be a great experience for all participants.

The Editorial Board:

---

Prof. Kazuo Yana

---

Prof. Jaakko Malmivuo

---

Prof. Steffen Leonhardt

## Contents

<b>Areas of Effectiveness of Defibrillating Pulse in the Energy/Phase Diagram for the Fibrillation Cycle on the Cardiomyocyte Model, <i>Boris Gorbunov, Vyacheslav Vostrikov, Igor Nesterenko and Dmitry Telyshev</i></b>	<b>1</b>
<b>Nonlinear Model Order Reduction of Thermoelectric Generator for Electrically Active Implants., <i>Onkar Jadhav, Cheng Dong Yuan, Evgenii Rudnyi, Dennis Hohlfeld and Tamara Bechtold</i></b>	<b>5</b>
<b>On the measurement of the dielectric properties of anisotropic biological tissues using electrical impedance, <i>Hyeuknam Kwon, Seward Rutkove and Benjamin Sanchez</i></b>	<b>8</b>
<b>The occlusive multichannel electrical impedance system of peripheral vein detection, <i>Mugeb Al-Harosh</i></b>	<b>12</b>
<b>Identification of acute coronary syndrome via body-surface mapping and inverse electrocardiography, <i>Scott B. Marrus, Menghao Zhang and R. Martin Arthur</i></b>	<b>15</b>
<b>Are Thigh and Calf Bioimpedance Spectroscopy less Susceptible to the Influence of Body Posture during Continuous Applications?, <i>Abdul Hamid Ismail, Carlos Castelar and Stefan Leonhardt</i></b>	<b>18</b>
<b>Investigation of ECG amplitude-phase coupling mechanisms, <i>Sergey Permyakov, Lyudmila Sushkova and Artemiy Kuznetshov</i></b>	<b>22</b>
<b>Noninvasive Detection of Magnetic Particles in Biological Nanomaterials using Magnetic Field Sensors, <i>Levan Ichkitidze, Sergei Selishchev and Michail Belodedov</i></b>	<b>26</b>
<b>Evaluation of the electrode system pressure force influence on neuromuscular activity signals, <i>Andrey Briko, Chvanova Julia, Alexander Kobelev and Sergey Shchukin</i></b>	<b>28</b>
<b>Body impedance spectroscopy based on processing of step response, <i>Uwe Pliquett, Ngoc Duc Nguyen, Dinh Yen Trinh, Thi Thuong Nguyen and Le Manh Hai</i></b>	<b>32</b>
<b>Zeta potential of cell surface - nanoenvironment interaction assessment, <i>Djamel Eddine Chafai, Ingrida Nemogová, Pavel Dráber and Michal Cifra</i></b>	<b>36</b>
<b>Real-time MEG data-processing unit for online medical imaging and brain-computer interface: a model-based approach, <i>Tao Chen, Sergey Suslov, Michael Schiek, Jürgen Dammers, N. Jon Shah and Stefan van Waasen</i></b>	<b>39</b>



<b>Peripheral Vascular Impedance Plethysmography for Respiratory Rate Estimation using Beat-to-Beat Features, <i>Michael Klum, Dennis Osterland, Alexandru-Gabriel Pielmus, Timo Tiggens and Reinhold Orglmeister</i></b>	<b>43</b>
<b>Arrhythmia Analysis in a Non-contact cECG Chair using Convolutional Neural Network, <i>Anake Pomprapa, Waqar Ahmed, André Stollenwerk, Stefan Kowalewski and Steffen Leonhardt</i></b>	<b>47</b>
<b>Development of an Electrical Phantom for Multi-Frequency Electrical Impedance Tomography based on the Visible Human Project, <i>Tobias Menden, Jakob Orschulik, Mazen Slimi, Steffen Leonhardt and Marian Walter</i></b>	<b>51</b>
<b>Bio-Impedance Analysis using Minimalistic Hardware, <i>Chris Gansauge, Danny Echtermeyer, Yahor Zaikou, Viktor Schroeder, Mario Saupe, Jörg Schemberg and Uwe Pliquet</i></b>	<b>55</b>
<b>Detection of Acute Respiratory Distress Syndrome using Sectoral Bioimpedance Spectroscopy - a Pilot Study, <i>Jakob Orschulik, Nadine Hochhausen, Susana Aguiar Santos, Michael Czaplík, Steffen Leonhardt and Marian Walter</i></b>	<b>59</b>
<b>Cerebrospinal fluid thermoimpedancemetry as a method of brain diseases diagnostics, <i>Viktoria Kapralova, Nataliya Vaskova, Evgeniy Shadrin, Aleksandr Ilinsky, Aleksandr Gryshkov and Birgit Glasmacher</i></b>	<b>63</b>
<b>Possibilities of joint application of acoustic radiation and direct magnetic field for biomedical research, <i>Igor Bondarenko, Oleg Avrunin, Aleksandr Gryshkov and Birgit Glasmacher</i></b>	<b>66</b>
<b>The distribution of the velocity and pressure fields in the nasal cavity at different respiration modes, <i>Yana Nosova, Oleg Avrunin, Natalia Shusliapina, Aleksandr Gryshkov and Birgit Glasmacher</i></b>	<b>68</b>
<b>Image processing for automated microscopic analysis of ice recrystallization process during isothermal annealing, <i>Maryna Prykhodko, Maksym Tymkovych, Oleg Avrunin, Vitalii Mutsenko, Aleksandr Gryshkov and Birgit Glasmacher</i></b>	<b>72</b>
<b>Bioimpedance spectro-tomography system using binary multifrequency excitation, <i>Mart Min, Mari Lehti-Polojärvi and Jari Hyttinen</i></b>	<b>76</b>
<b>Development of a test bench for the characterization of movement artifacts in smart textile systems, <i>Akram Idrissi, Malte Kaiser, Simon Albrecht, Sebastian Richert, Thomas Gries and Andreas Blaeser</i></b>	<b>80</b>
<b>Microgravity effect and efficacy of high intensity jump training on default mode network alterations during light sleep on extreme environments, <i>Christos Frantzidis, Christina Plomariti, Sotiria Gilou, Polyxeni Gkivogkli, Dimitris Fotopoulos, Giorgos Ntakakis, Evangelos Paraskevopoulos, Chrysoula Kourtidou-Papadeli and Panagiotis Bamidis</i></b>	<b>84</b>
<b>The electrical impedance method of the muscle blood supply definition in damaged intervertebral discs area, <i>Andrew Blinow and Sergey Shchukin</i></b>	<b>88</b>
<b>An engineer's approach: How can 10-100 <math>\mu</math>T, 10-100 Hz magnetic field influence human cardiovascular regulation?, <i>Joël Niederhauser</i></b>	<b>92</b>

**Pilot Characterization of Human Bones by Spectroscopic Techniques, *Angelica Hernandez Rayas, Francisco Vargas Luna, Teodoro Cordova Fraga, Martha Hernández Gonzalez, Nicolás Padilla Raigoza and Octavio Jiménez Gonzalez*** 96

**Inter-modal and Intra-modal interference in a Multi-Modal Sensor for Non-contact Monitoring of Vital Signs in Patient Beds, *Xinchi Yu, Wilko Neu, Pascal Vetter, Cornelius Bollheimer, Steffen Leonhardt and Daniel Teichmann*** 99

Proceedings of the 11<sup>th</sup> International Conference on Bioelectromagnetism 2018, Aachen, Germany, © 2018, International Society for Bioelectromagnetism (ISBEM)

# The distribution of the velocity and pressure fields in the nasal cavity at different respiration modes

Ya.V. Nosova<sup>1</sup>, O.G. Avrunin<sup>1</sup>, N.O. Shusliapina<sup>2</sup>, O. Gryshkov<sup>3</sup>, B. Glasmacher<sup>3</sup>

<sup>1</sup>Kharkiv National University of Radioelectronics, Nauki Avenue 14, Kharkiv, Ukraine

<sup>2</sup>Kharkiv National Medical University, Nauki Avenue 4, Kharkiv, Ukraine

<sup>3</sup>Institute for Multiphase Processes, Leibniz Universität Hannover, Callinstr. 36, Hannover, Germany

Contact: [oleh.avrunin@nure.ua](mailto:oleh.avrunin@nure.ua), [gryshkov@imp.uni-hannover.de](mailto:gryshkov@imp.uni-hannover.de)

## Introduction

Topical are the problems associated with the prediction and evaluation of the functional results of endonasal surgery, which, in the case of respiratory and olfactory disorders [1-3], are the condition of air passage through the superior nasal passage and the restoration of olfactory sensitivity.

Changing the direction of the main air stream with nasal breathing leads to constant irritation of certain sections of the mucosa membrane (for example, a portion of the mucosa of the nasal cavity that contains olfactory receptors, the so-called olfactory zone), which will subsequently lead to cellular infiltration in this region and then to hypertrophy of the mucosa shell. Therefore, it is necessary to study the distribution of velocities and pressures in the nasal cavity under different respiration regimes.

## Materials and Methods

An important characteristic of nasal breathing is the distribution of air flow rates along the sections of the nasal cavity. When analyzing the existing approaches, it was determined that the main method of studying the aerodynamics of the nasal cavity is rhinomanometry. However, there is not always a clear correlation between anatomical and functional indicators, as well as subjective feelings of the patient and rhinomanometric data [4-9]. Numerical modeling of air passage through the nasal cavity is also used with the help of special applications that allow one to observe animated and static flow patterns on the computer screen, as well as integral air flow indicators, updated after each global iteration (changes in the flow structure as a function of time). The most famous and functional software packages are CFX (Canada, Great Britain, Germany), Ansys, Flotran module, (USA), STAR-CD (Great Britain), Fluent (USA), Numeca (Belgium), Flow-ER (Ukraine), Flow Vision (Russia).

Calculation of gas flow in modern software products is performed by numerically solving a system of equations describing the most general case of motion of a liquid medium. These are the Navier-Stokes equations and continuity. The boundary conditions, as a rule, are conditions for the flow velocity to be zero on the walls of the cavity, the distribution of velocity components in the input section and the zero of the first derivatives (in the direction of flow) of the velocity components in the outlet section, it is also possible to specify the average flow velocity or flow rate. The output parameters are not specified. The pressure enters the equation only in the form of the first

derivatives, and its value is indicated only at one point in the computational domain. The most frequent phenomena in biological objects are turbulent currents. Direct simulation of turbulent flows by numerical solution of the Navier-Stokes equations written for instantaneous velocities is still extremely difficult, and, as a rule, not instantaneous, but averaged values of the velocities are of practical interest. Often, for the analysis of turbulent flows, instead of equations, the Reynolds equations and various models of turbulence are used.

The choice of the software package FlowVision for numerical modeling of aerodynamic processes in the nasal cavity is due to its availability in the Ukrainian software market, as well as the dissemination of its non-commercial versions (using an unlimited demo version of FlowVision 2 with a limited grid capacity of 15,000 cells).

However, the software product FlowVision does not have an embedded preprocessor (its own development tools for creating geometric objects), but it allows one to import the geometric configuration of the investigated structures (cavities) from many modern CAD-systems, for example, SolidWorks, Compass 3D, AutoCAD. Also, the package has a convenient interface that allows one to visualize the imported calculation area, specify the boundary conditions, environment properties, and the parameters to be examined. The FlowVision package uses a rectangular (Cartesian) design grid with the ability to adaptively select cell sizes and an approach to discretizing the equations of a mathematical model based on the finite volume method that provides the law of conservation of integral quantities (flow, momentum) in each of the computational grid cells. In this case, a certain closed region of gas flow is selected for which the fields of macroscopic quantities (for example, pressure drop, velocity, flow) are searched, describing the state of the medium in time and satisfying certain physical laws.

Convenient post-processing tools allow one to watch animated and static flow patterns on the screen, as well as integral flow indicators that are updated after each global iteration (changing the flow structure as a function of time). The set of available visualization tools includes standard two-dimensional graphics, vector fields, isolines and isosurfaces of the specified parameters, color filling of regions depending on the values of the parameter being studied, and animation of the motion of the fluid particles. After loading in the software package of the geometric model of the upper respiratory tract in \*.STL format, the following parameters were specified:

1. Setting of the properties of the calculation area and parameters of the medium
2. Setting of boundary conditions (the value of the pressure differential on the nasal cavity (0.3, 1.0, 2.0, 5.0 and 10 kPa)
3. Introduction of flow through the nasal cavity (0.3, 0.6, 1, 2 and 4 s<sup>-1</sup>), velocity at the wall equal to zero), type and additional parameters of the computational model.

## Results

For a laminar regime in a section with radius  $a$ , we obtain a parabolic dependence of the velocities  $W$  on the distance from the center  $r$ :

$$W = 2W \left( 1 - \frac{r^2}{a^2} \right) \quad (1)$$

where  $W$  is the average speed,  $r$  is the distance from the center, and  $a$  is the radius

For the turbulent regime, the velocity is defined as follows:

$$U = U_{max} \left( \frac{r}{a} \right)^{0.9\sqrt{\lambda}} \quad (2)$$

where  $U_{max}$  is the maximum speed,  $\lambda$  is the loss factor.

Numerical data on the distribution of airflow velocities with an accuracy of 15% coincide with the analytical solutions obtained by equations (1, 2).

Whatever the law of velocity distribution in the section of the turbulent flow, the speed near the wall is 0, increasing to the axis of the flow. Consequently, there should be a low-speed layer, the thickness of which depends on Reynolds number  $Re$ , and the velocity increases from 0 to 90% of the velocity of the core of the flow (fig. 1) [4-6].

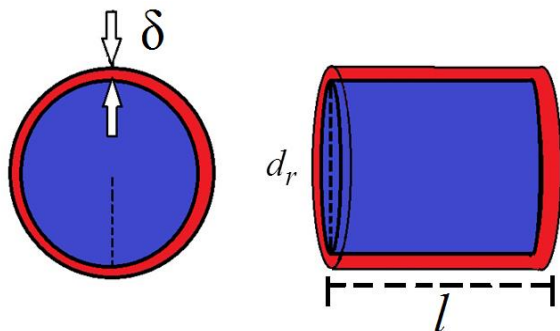


**Figure 1:** Schematic representation of the turbulent core of the stream (blue) and laminar boundary layer (red color) ( $d_r$  – is the hydraulic diameter,  $\delta$  – the thickness of the laminar boundary layer,  $l$  – length of section)

With an increase in airflow velocity (with forced breathing-physical load, narrowing of the nasal passage), the thickness of the laminar boundary layer will decrease, the mucosa will be exposed to high-speed turbulent flow. Turbulization of the air flow will promote drying of individual areas of the mucous membrane of the nasal cavity, and as a result traumatization of the mucosa with subsequent morphological rearrangement of individual areas.

In the laminar regime, the highest velocity is observed in the central regions of the general and inferior nasal passages. In the turbulent regime, the velocity is also constant over a larger cross-sectional area and the velocity in the near-wall region is sharply reduced.

Air flow rates corresponded to 0.2, 1 and 2 L/s (calm, strengthened and forced - with physical exertion). The values of the distribution of the pressure difference were in the range 0.1-5 kPa - the upper limit characterizes the regime of forced breathing. The air flow rates were dependent on the nasal cavity sections in the range from 0.04 to 3 m/s, with maximum velocities observed in the nasal valve region and in the anatomical narrowing of the canal. With pronounced local resistances, the results of numerical simulation clearly showed areas of increased turbulence and swirl up to the reverse flow. These processes, leading to difficulty in nasal breathing, were clearly visualized with an aerodynamic drag coefficient greater than 1.5 kPa l/s.

The Reynolds numbers (fig. 2 c, d and fig. 3 c, d) depend essentially on the degree of forced breathing, and on the equivalent diameter and area of the nasal cavity and, in fact, mirror the distributions of the corresponding parameters. With quiet breathing (flow rate 0.5 l/s), the Reynolds numbers are small for almost all the cases under consideration (fig. 2 c, d and fig. 3 c, d) and sharply increase to 10,000 or more with forced respiration (at a flow rate of 2 l/s) and have extremes in generalized, or local narrowing of the nasal canals. Increased Reynolds numbers indicate an increase in turbulence in the corresponding areas of the nasal cavity.

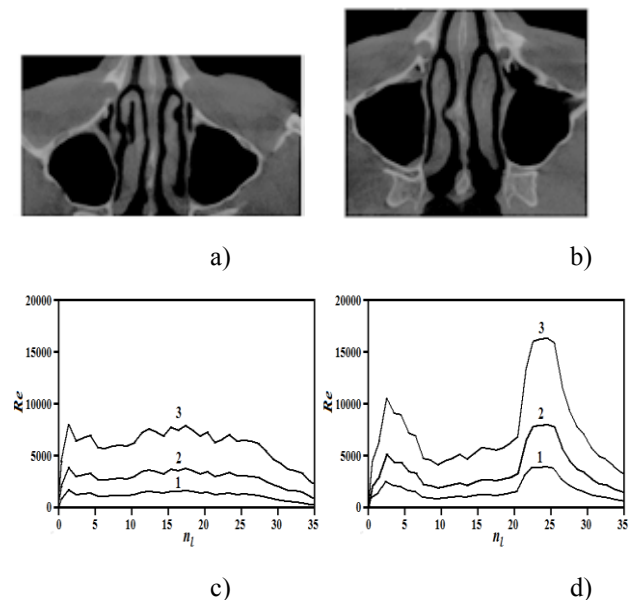


**Figure 2:** Images of characteristic axial SCT sections: a) without disturbance of nasal breathing; b) when the nasal septum is curved to the right; and the corresponding distributions for the right nasal passage: c), d) Reynolds numbers along the length of the nasal cavity at costs of 0.5 (1), 1.0 (2) and 2.0 (3) l/s ( $n$  – numbers of the frontal sections of the nasal cavity)

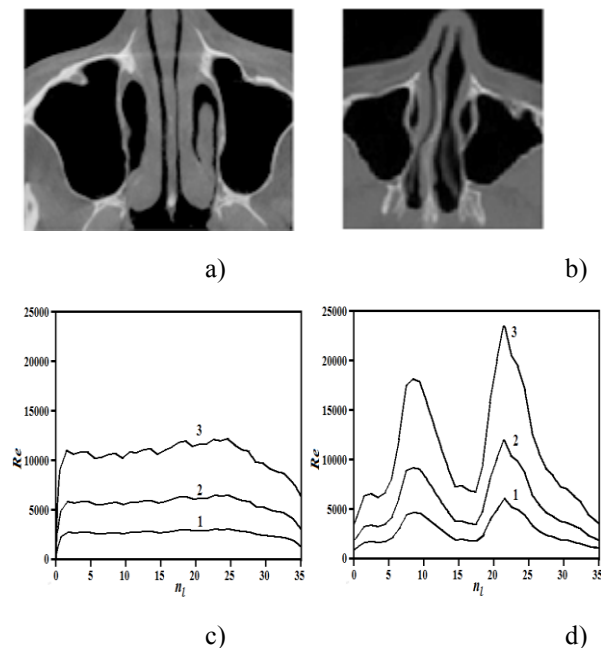


**Figure 3:** Images of characteristic axial SCT sections: a) in chronic rhinosinusitis, b) with S-shaped wavy curvature of the nasal septum; and the corresponding distributions for the right nasal passage c), d) of the Reynolds numbers along the length of the nasal cavity at flow rates of 0.5 (1), 1.0 (2) and 2.0 (3) 1/s ( $n$  - numbers of the frontal sections of the nasal cavity)

## Discussion

Spatial mapping of the model of air passage through the nasal cavity, shown in fig. 4, allows one to visually estimate the air flow rate in the density of streamlines and in the animation mode to estimate the airflow velocity in different parts of the upper respiratory tract. The visualization of data on the pressure drop along the length of the nasal cavity is shown in fig. 5 - the pressure values will be constant across sections, which are isobaric planes. The errors of the averaged analytical and numerical method with respect to the calculation of the pressure in the sections of the nasal cavity are within 10%.

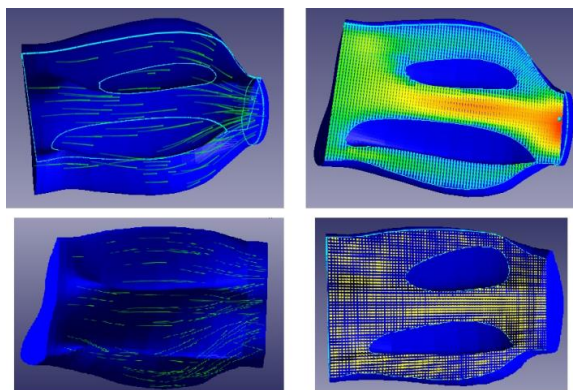


**Figure 4:** An illustration of the velocity field along the nasal passage (by the density of the airflow lines) from the data of the numerical experiment in the FlowVision package

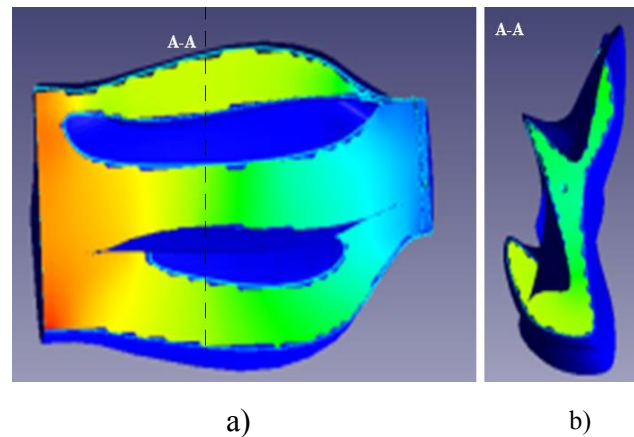


**Figure 5:** The distribution of pressure drop along the length of the nasal passage according to the data of the numerical experiment in the FlowVision package: a - along the sagittal section of the nasal passage; b - in one of the characteristic sections (AA) of the nasal passage (half-tones illustrate the change in pressure drop)

## Conclusions

Thus, the three-dimensional modeling of the air flow through the nasal cavity allows to map the nasal passages along the parameters studied and to study their local values, which is important for the planning of minimally invasive surgical interventions. However, the numerical modeling of the air flow in the nasal cavity with the help of software packages requires a large time (up to several working days), which is associated with a rather cumbersome stage of preparing the initial data. This includes interactive segmentation of anatomical objects, tracing contours of airborne structures, forming a three-dimensional model nasal moves and its subsequent loading into the simulation environment, eliminating model geometry errors, often resulting in repeated iterative implementation of the pre-stages and direct modeling stage, during which an aerodynamic and a large number of imaging parameters.

Analytical decisions are rather simplistic, but in most cases allow to adequately assessing the degree of nasal aerodynamics disturbance. In fact, this is an extended model of a one-dimensional flow of air in a channel in a complex form, in which the geometric characteristics of the nasal cavity are taken into account by the hydraulic diameter. Preparation for the construction and analysis of the numerical model is a much more labor-intensive process, but allows you to visualize detailed spatial patterns of the distribution of aerodynamic parameters (3d fields of velocities and pressure drops), which allows you to visualize reverse currents.

## References

- [1] C. Manesse, C. Ferdenzi, M. Sabri, *et al.* Dysosmia-Associated Changes in Eating Behavior. *Chem Percept*, 10:104, 2017, doi:10.1007/s12078-017-9237-3
- [2] Nosova Ya., Avrunin O., Semenets V. Biotechnical system for integrated olfactometry diagnostics. *Innovative technol-*



- ogies and scientific solutions for industries, 1(1):64–68, 2017.
- [3] S. Boesveldt, S.T. Lindau, M.K. McClintock, T. Hummel, J.N. Lundström. Gustatory and olfactory dysfunction in older adults: a national probability study. *Rhinology*, 49(3): 324–330, 2011
- [4] I-C. Chen, Y-T. Lin, J-H. Hsu, Y-C. Liu, J-R. Wu, Z-K. Dai. Nasal Airflow Measured by Rhinomanometry Correlates with FeNO in Children with Asthma. *PLoS ONE*, 11(10): e0165440, 2016, doi: 10.1371/journal.pone.0165440
- [5] M. M. Tavakol, E. Ghahramani, O. Abouali, M. Yaghoubi, G. Ahmadi. Deposition fraction of ellipsoidal fibers in a model of human nasal cavity for laminar and turbulent flows. *J Aerosol Sci*, 113: 52-70, 2017
- [6] N. Curle. *The Laminar Boundary Layer Equations*. Courier Dover Publications, 176, 2017
- [7] J.-H. Lee, Y. Na, S.-K. Kim, S.-K. Chung. Unsteady flow characteristics through a human nasal airway. *Respir Physiol Neurobiol* 172(3): 136-146, 2010
- [8] O. Avrunin. Extended of diagnostic capabilities for the Rhinomanometry method. In O. Avrunin, N. Shuslyapina, J. Ivanchenko, 5.1: 315-321. Spatial aspects of socio-economic systems' development: the economy, education and health care. Monograph. Opole: The Academy of Management and Administration in Opole.- Publishing House WSZiA, 2015, ISBN 978-83-62683-64-0. – 380.
- [9] Y. Nosova, N. Shushliapina, S.V. Kostishyn, L.G. Koval, Z. Omiotek, *et al.* The use of statistical characteristics of measured signals to increasing the reliability of the rhinomanometric diagnosis. *Proc. SPIE 10031, Photonics Applications in Astronomy, Communications, Industry, and High-Energy Physics Experiments 2016*, 100312M (September 28, 2016); doi:10.1117/12.2248364
- [10] H.F. Ismail, E. Osman, A.K. AL-Omari, O.G. Avrunin. The Role of Paranasal Sinuses in the Aerodynamics of the Nasal Cavities. *International Journal of Life Science and Medical Research*, 2(3): 52-55, 2012

## Acknowledgements

The authors acknowledge the exchange program with East European Countries funded by DAAD (project number 54364768). We also thank Kalashnik M.V and the staff of the otorhinolaryngological department of the Kharkov regional hospital for assisting in experiments and validating the results.